Supplementary Material

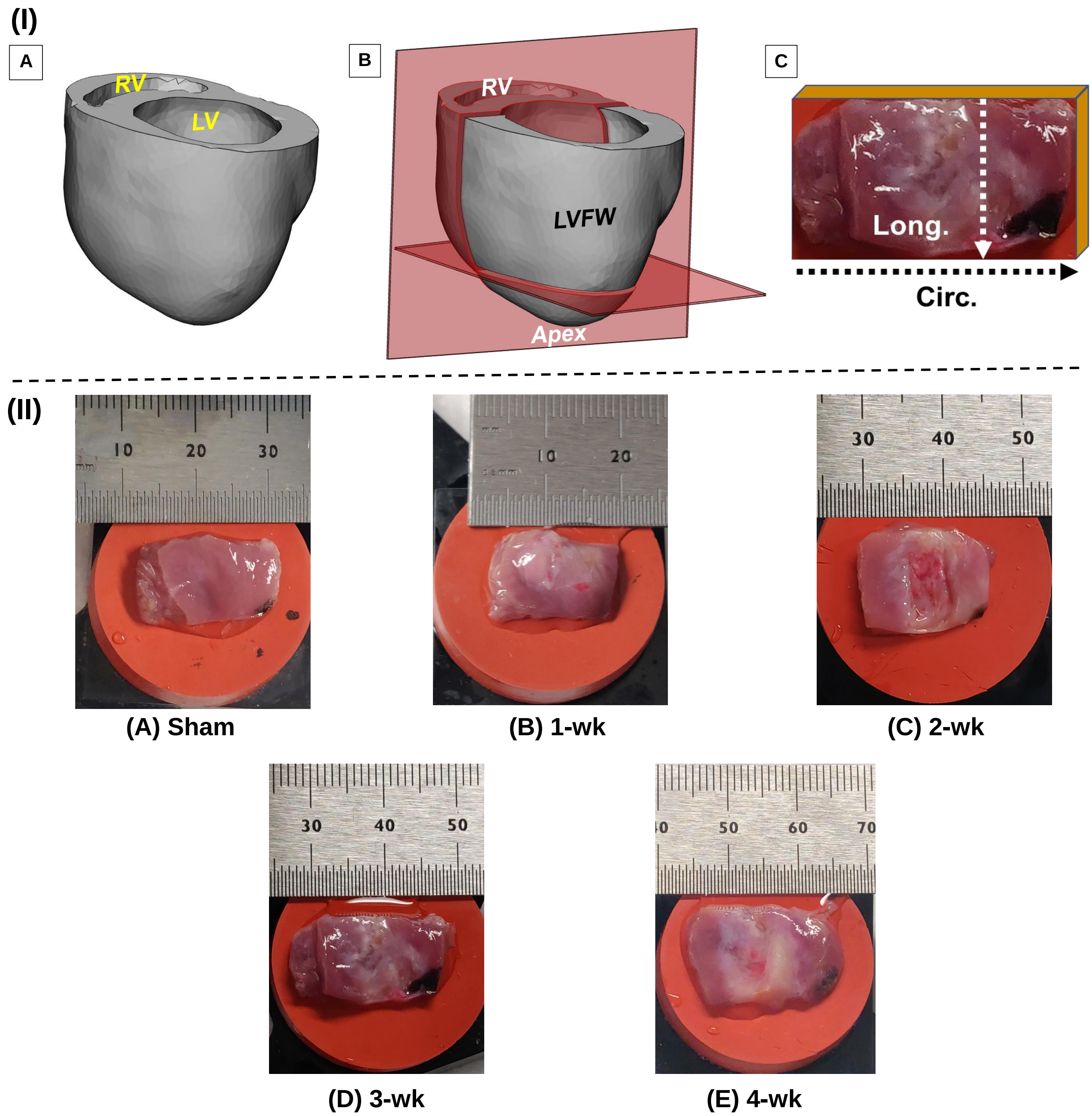

Figure 1. (**I**) Schematics indicating the isolation of the full LVFW from the left ventricle: (**A**) Representative structure of a truncated. (**B**) Isolation of the LVFW by removing the right ventricle (RV), inter-ventricular septum, and a small part of the apex. (**C**) A representative excised LVFW specimen. (**II**) LVFW of representative rodent specimens from control and infarct groups at four timepoints post-MI. The ruler indicates measurements in millimeters.

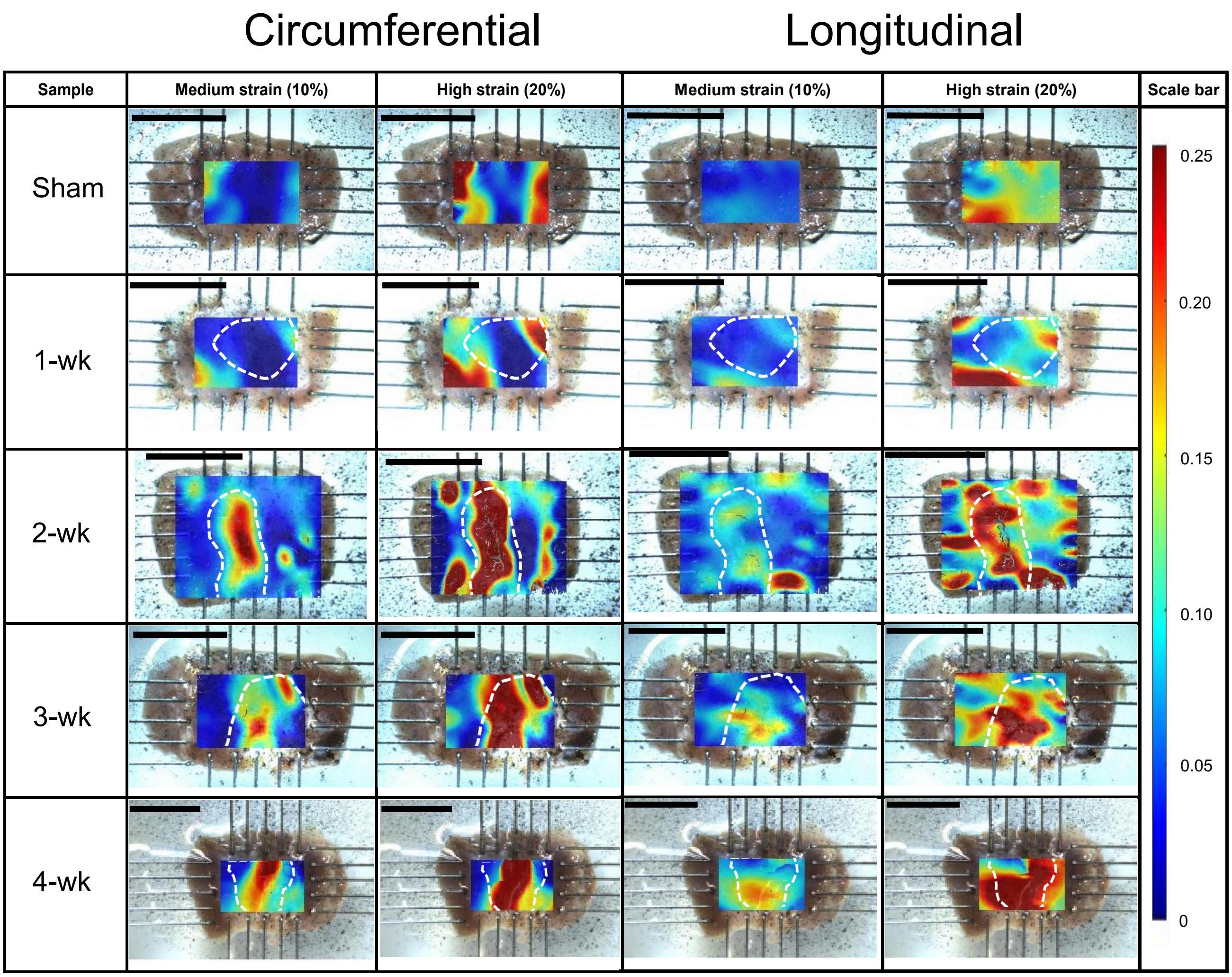

Figure 2. Regional strain obtained from digital image correlation at 10 and 20% strain. Scale bars indicate 10 mm.

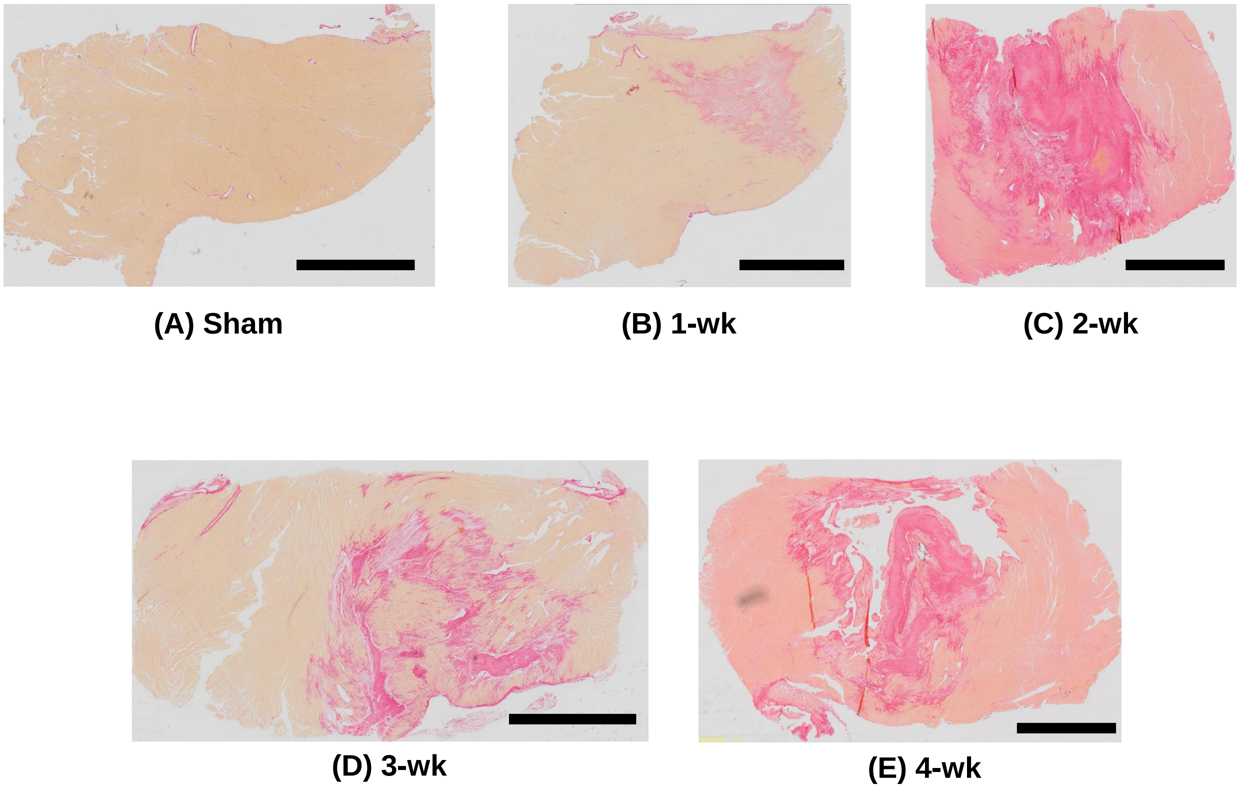

Figure 3. Representative histological images using picrosirius red (PSR) staining at various timepoints. The yellow/orange regions indicate myofiber content and the pink/red regions indicate collagen content. Scale bar: 5 mm.

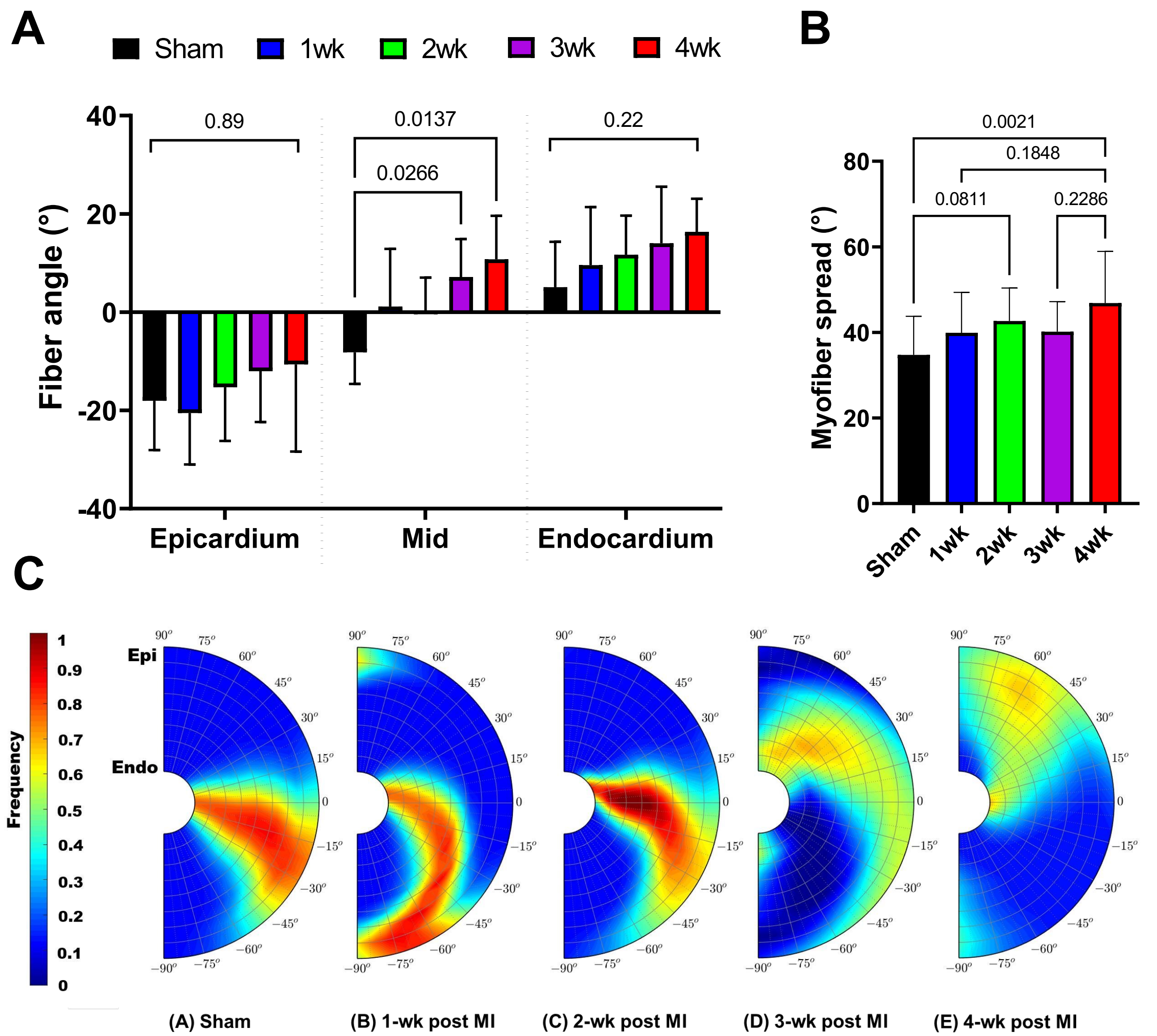

Figure 4. **(A)** Mean myofiber angle at several transmural depths. **(B)** Mean myofiber spread of the entire LVFW at various post-MI timepoints.**(C)** Representative myofiber orientation plots for each timepoint. The radial direction indicates the transmural depth and the tangential direction indicates the myofiber orientation angle. The inner circle represents the endocardium while the outer circle represents the epicardial surface. Statistical significance was calculated by performing ordinary one-way ANOVA with Tukey's multiple comparison test. n=6 at each timepoint.

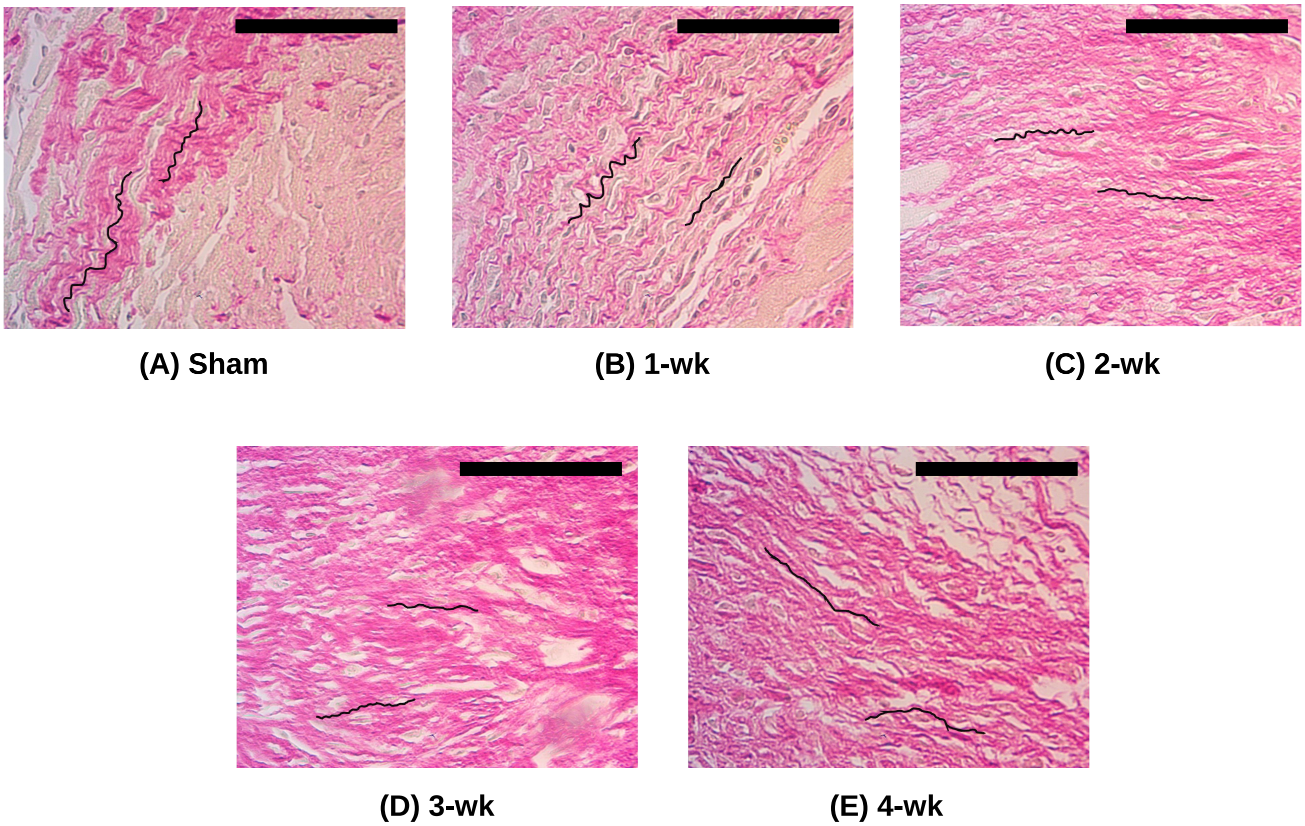

Figure 5. Representative images of the collagen undulation observed with the progression of remodeling. Black lines are used to highlight representative collagen fiber undulation. Scale bar - 100μm.

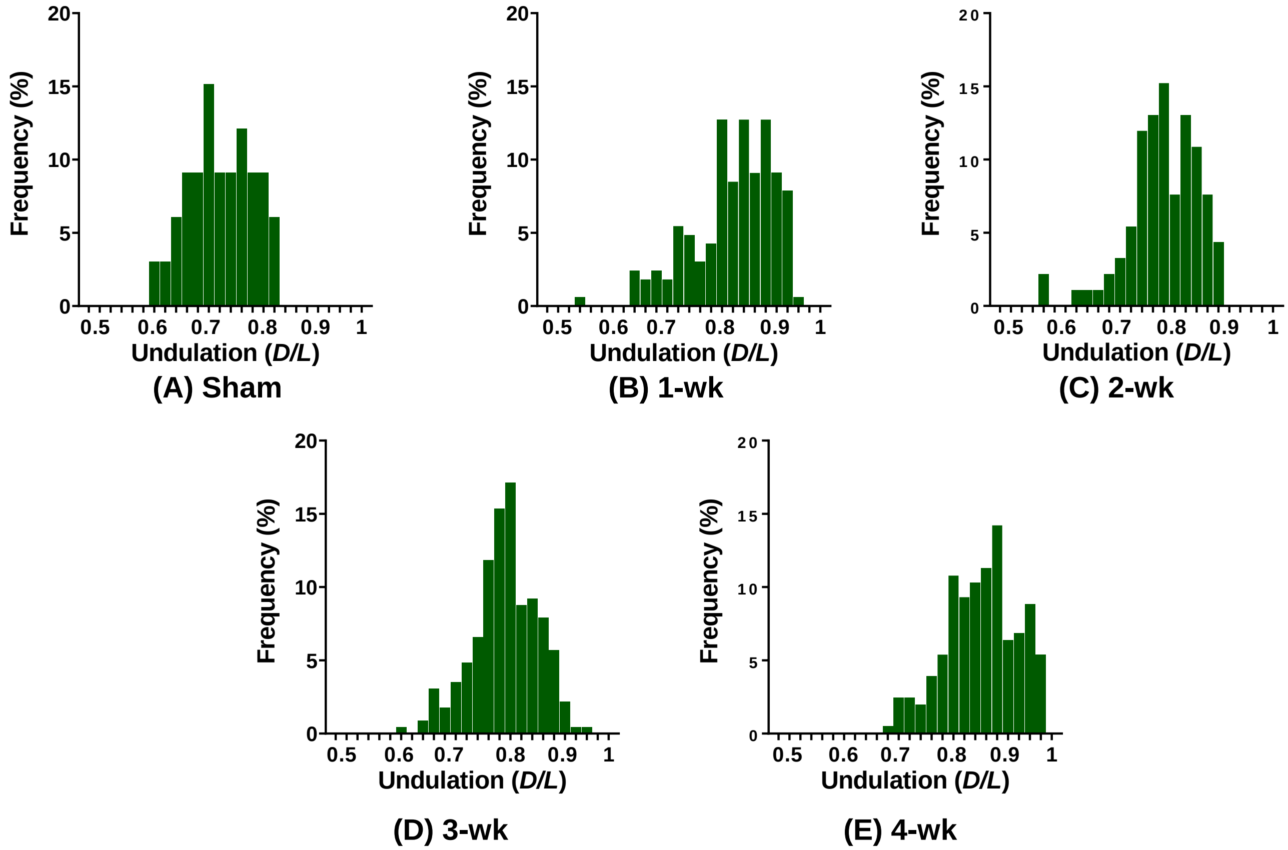

Figure 6. Representative distribution of collagen undulation at each timepoint. Note that the extreme undulation values of 0 and 1 correspond to an entirely coiled and a perfectly straight (taut) fiber, respectively.

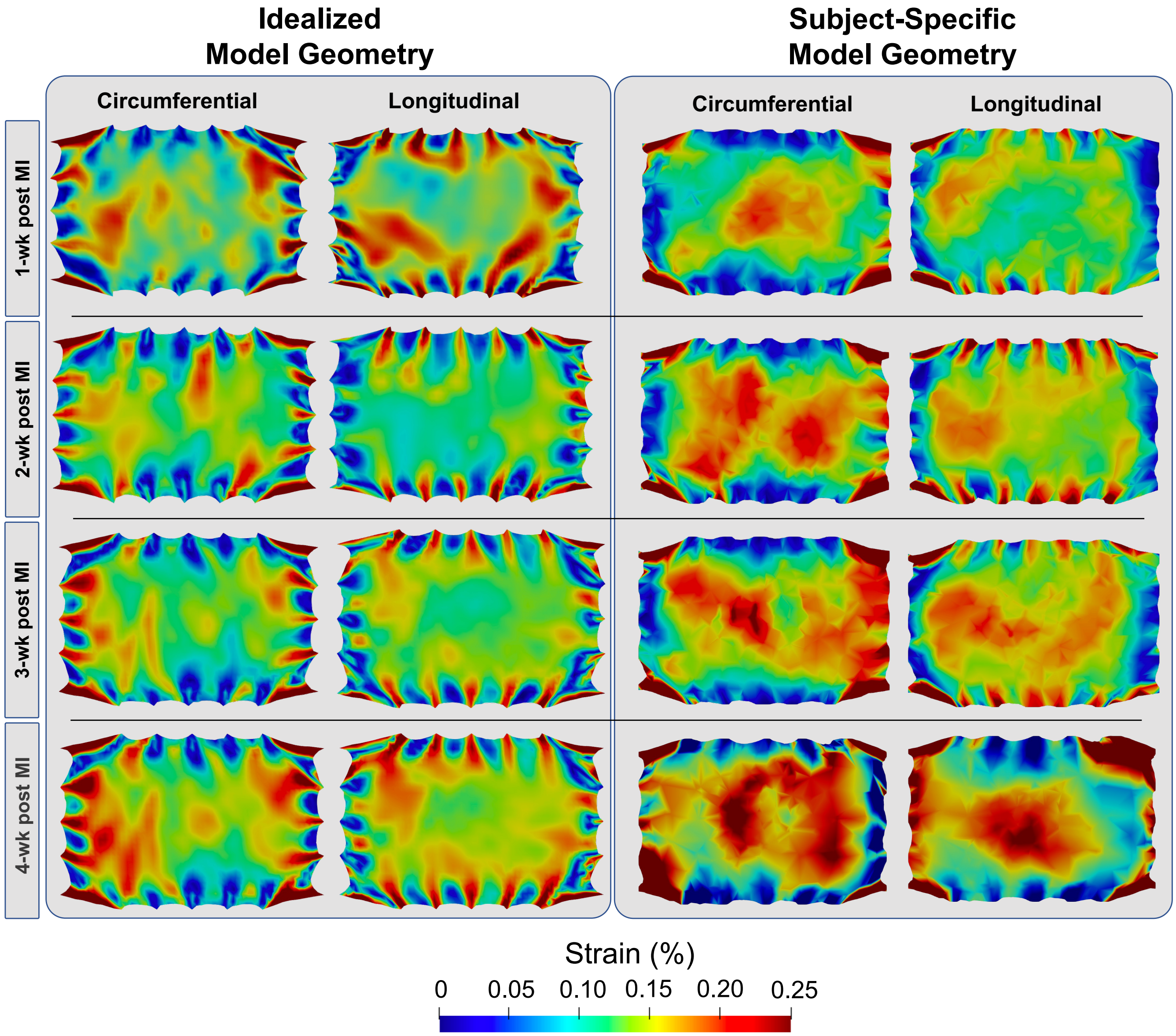

Figure 7. Simulated circumferential and longitudinal strain distributions visualized at all post-MI timepoints. Visualizations in the left panel are predictions from finite-element models with idealized rectangular geometry while those in the right panel are predictions from models which incorporate a subject-specific regional variation in geometry thickness. Regional strains are reported at 20% external strain and visualized at a central 2-D cross-section.

Table 1. Mean and standard deviation of regional circumferential and longitudinal strain calculated from digital image correlation.

	Infarct		Remote	
	Circumferential	Longitudinal	Circumferential	Longitudinal
Sham	-	-	0.161 ± 0.137	0.149 ± 0.064
1-wk	0.113 ± 0.747	0.1304 ± 0.028	0.066 ± 0.064	0.086 ± 0.039
2-wk	0.227 ± 0.293	0.162 ± 0.067	0.193 ± 0.205	0.150 ± 0.066
3-wk	0.229 ± 0.082	0.179 ± 0.047	0.141 ± 0.128	0.136 ± 0.095
4-wk	0.204 ± 0.099	0.283 ± 0.186	0.127 ± 0.138	0.154 ± 0.127

Table 2. Percent change in optimized parameter values after introduction of white Gaussian noise to the fitting data.

	a_m (kPa)	a_c (kPa)
Sham	7.1	-6.2
1-wk	2.0	-2.2
2-wk	-5.2	-7.7
3-wk	-5.1	3.7
4-wk	-2.6	9.1

Table 3. Comparison of mean circumferential strain in remote and infarct regions between models with idealized geometry and subject-specific regional thickness.

	Idealized Geometry		Subject-specific Geometry	
	Infarct	Remote	Infarct	Remote
Sham	-	0.122 ± 0.082	-	-
1-wk	0.139 ± 0.116	0.133 ± 0.068	0.177 ± 0.189	0.170 ± 0.119
2-wk	0.132 ± 0.076	0.130 ± 0.057	0.167 ± 0.140	0.160 ± 0.107
3-wk	0.130 ± 0.112	0.132 ± 0.063	0.205 ± 0.185	0.156 ± 0.122
4-wk	0.148 ± 0.098	0.139 ± 0.066	0.170 ± 0.144	0.160 ± 0.130

Table 4. Comparison of mean longitudinal strain in remote and infarct regions between models with idealized geometry and subject-specific regional thickness.

	Idealized Geometry		Subject-specific Geometry	
	Infarct	Remote	Infarct	Remote
Sham	-	0.110 ± 0.107	-	-
1-wk	0.156 ± 0.124	0.130 ± 0.065	0.190 ± 0.227	0.165 ± 0.129
2-wk	0.124 ± 0.070	0.115 ± 0.055	0.178 ± 0.152	0.153 ± 0.104
3-wk	0.150 ± 0.089	0.128 ± 0.055	0.219 ± 0.218	0.158 ± 0.124
4-wk	0.142 ± 0.073	0.132 ± 0.060	0.182 ± 0.149	0.151 ± 0.114